Improving quantum-battery lifetime by the electromagnetically-induced-transparency effect and bound states

Jin-Tian Zhang, Cheng-Ge Liu, and Qing Ai[*]

School of Physics and Astronomy, Applied Optics Beijing Area Major Laboratory, Beijing Normal University, Beijing 100875, China
and Key Laboratory of Multiscale Spin Physics, Ministry of Education, Beijing Normal University, Beijing 100875, China

Quantum battery (QB) is an application of quantum thermodynamics which uses quantum effects to store and transfer energy, overcoming the limitations of classical batteries and potentially improving the QB's performance. However, due to the interaction with the external environment, it leads to decoherence and thus reduces both the lifetime and the charging efficiency of QB. Here, we propose suppressing the environmental dissipation in the energy-storage process of the QB by exploiting both the electromagnetically-induced-transparency (EIT) effect and bound states. By constructing a hybrid system composed of a four-level atom and a coupled-cavity array, two bound states are formed in the system when the energy of the QB is in the energy band of the cavity array. Environmental dissipation is significantly inhibited due to the bound state and EIT effects, which extends the lifetime of the QB. We show that the charging efficiency of the QB is optimal when the energy of the QB is in resonance with the cavity. In addition, there is an optimal coupling strength between the two adjacent cavities, which helps to improve the performance of the QB. Our research has achieved the realization of long-term energy storage while improving the charging efficiency of QB, which has practical implications for the realization of QB.

I. INTRODUCTION

In recent decades, due to the application of nanomechanical electronic devices, quantum technology has gradually attracted broad interest [1,2]. Quantum thermodynamics focuses on the transfer and storage of energy at the nanoscale [3–7]. It studies work and entropy in a quantum context [8–11]. The laws of classical thermodynamics have been reconsidered to describe heat engines and energy-storage systems based on quantum effects, breaking the limits of classical physics [12–15]. As a nanoscale energy storage and conversion device, the aim of the design of the quantum battery (QB) is fundamentally different from that of conventional batteries by exploiting the properties of quantum thermodynamics [16–18].

The QBs utilize quantum effects such as entanglement [16,19–22] and coherence [23–26] to achieve charging power and battery capacity higher than those of their classical counterparts [17,27–29]. The basic mechanism underlying the QBs is that, for example, a two-level system acts as a QB and another two-level system [30–33] or external field acts as a charger [34–37]. Here, due to their interaction, the energy can be coherently transferred between the charger and the QBs and thus results in the charged QBs. It has been experimentally demonstrated that charging of the QBs can be achieved in various physical systems including nuclear magnetic resonance [38], superconducting circuits [39,40], photonic systems [41], and organic microcavities [42]. An

efficient QB scheme is essential for its implementation and future applications, e.g., utilizing the collective-excitation mode [43] and a one-dimensional dimerized *XY* chain as a spin QB [44]. Since the realization of the QB has generally been considered in the context of open quantum systems [45,46], a serious problem for QB may occur. Due to the decoherence caused by the external environment, the charging efficiency of the QB will be reduced, and the stored energy will be depleted [47]. Various methods have been proposed to beat the dissipation, e.g., feedback control [48] and Floquet engineering [49]. However, how to improve the charging efficiency of QBs while supressing the decoherence caused by the external environment is an intriguing challenge.

As known to all, electromagnetically-induced transparency (EIT) is a quantum-coherence phenomenon [50], which is widely observed in atomic or molecular systems. When a probe field passes a medium with resonant two-level atoms, i.e., the ground state and a lossy excited state, the transmittance of the probe field will significantly decrease due to the absorption. However, if a control field is introduced to induce the transition between the lossy excited state and a metastable state, the probe field will pass the medium as if it is transparent, and thus it is called EIT. There are typically three kinds of configurations for the EIT, i.e., the ladder type, the V-type, and the Λ type [51]. In the EIT, there exists a dark state, i.e., the superposition of the ground state and the metastable state [52]. Due to the dark state being void of the lossy excited state, the probe field can pass the medium without absorption. The dark state has been applied in different physical processes, e.g., coherent energy transfer of artificial light harvesting [53] and perfect state transfer in optomechanical systems [54,55].

043705-1

Recently, remote charging and degradation suppression of the QB has been proposed when bound states form in the total system including the charger, the QB, and the electromagnetic field [56,57]. In this work, inspired by these discoveries, we theoretically propose a QB scheme utilizing a hybrid system composed of a four-level atom as the QB and a coupled-cavity array as the charger, which can be implemented with superconducting transmission line resonators [58–61] and a superconducting charge qubit [62,63]. By applying two coherent light beams to the four-level atom, we can realize a quasi-two-level system with a dark state and the ground state for the QB. We show that the interaction between the dark state of the QB and the coupled-cavity array gives rise to two bound states in the hybrid system. Remarkably, the bound states assisted by the dark state significantly suppress the environmental dissipation, thereby enhancing the QB's lifetime. Furthermore, our results reveal that the extractable work, i.e., the ergotropy, reaches its maximum when the dark state is resonant with the bare frequency of the cavity. We further demonstrate that the coupling strength between adjacent cavities can be optimized to enhance the performance of the QB. Unlike in the traditional dark-state QB [37,46,64,65], we propose a charging and energy-storage mechanism that integrates the effects of the EIT with the formation of bound states. The introduction of EIT not only enhances the coherence between the QB and its environment but also facilitates the formation of the dark state. These special states including the bound states can significantly extend the lifetime of the QB while simultaneously improving its charging efficiency.

This article is structured as follows. In the next section, we introduce our QB protocol. By using the dark state, we obtain the effective Hamiltonian of the QB interacting with the coupled-cavity array, as derived in detail in Appendix A. It is demonstrated that the eigenenergies of the bound states determine the quantum dynamics of the dark state, with its detailed derivation shown in Appendix B. Then, in Sec. III, we perform numerical simulations. The relationship between the number of bound states and the energy of the dark state is explored. We use both analytical and numerical methods to verify that, in the presence of two bound states, environmental dissipation can be significantly suppressed due to the combination of the bound states and the dark state. The charging efficiency of the QB is optimal when the energy of the QB is in resonance with the cavity. In Sec. IV, we summarize our main findings.

II. SCHEME

To study the effects of the environmental dissipation on the energy storage process of a QB, we consider the interaction between a four-level atom and a coupled-cavity array. As shown in Fig. 1, we make use of the four-level atom as a tool for energy storage, i.e., a QB, and the coupled N cavities as a medium for energy transfer. The Hamiltonian of the system reads

$$H = H_c + H_B + H_I, \tag{1}$$

$$H_c = \sum_j \omega_0 a_j^\dagger a_j - \xi \sum_j (a_j^\dagger a_{j+1} + a_{j+1}^\dagger a_j), \tag{2}$$
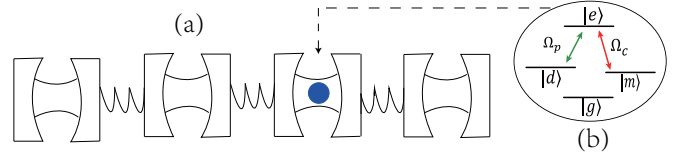

FIG. 1. Schematic illustration of the charging QB model. (a) Structure of coupled cavities. (b) A four-level atom, where $|d\rangle$ is a metastable energy level, $|m\rangle$ is a auxiliary energy level, and $|e\rangle$ is an excited state energy level. Two pulses are applied at the same time to induce the transitions of $|e\rangle \leftrightarrow |d\rangle$ and $|e\rangle \leftrightarrow |m\rangle$ with, respectively, Rabi frequencies Ω_p and Ω_c.

$$H_B = \Omega_d|d\rangle\langle d| + \Omega_e|e\rangle\langle e| + \Omega_m|m\rangle\langle m| \\ + \Omega_p e^{-i\omega_p t}|e\rangle\langle d| + \Omega_c e^{-i\omega_c t}|e\rangle\langle m| + \text{H.c.}, \tag{3}$$

$$H_I = g_1 a_0^\dagger|g\rangle\langle d| + g_2 a_0^\dagger|g\rangle\langle m| + \text{H.c.}, \tag{4}$$

where $a_j^\dagger$ (a_j) represents creation (annihilation) of a photon with frequency ω_0 in the jth cavity; ξ is the coupling constant between two neighboring resonators; Ω_d, Ω_e, and Ω_m are respectively the transition frequencies of the four-level atom from $|g\rangle$ to $|d\rangle$, $|e\rangle$, and $|m\rangle$. Between the energy levels $|d\rangle(|m\rangle)$ and $|e\rangle$, we apply a probe (control) light with the driving frequency $\omega_{p(c)}$ and the Rabi frequency $\Omega_{p(c)}$. $g_1(g_2)$ is the coupling constant between the transition $|g\rangle \leftrightarrow |d\rangle(|g\rangle \leftrightarrow |m\rangle)$ and the 0th cavity. In this article, we have assumed $\hbar = 1$ for simplicity. Here, we apply the classical drivings which are respectively in close resonance with the transitions $|e\rangle \leftrightarrows |d\rangle$ and $|e\rangle \leftrightarrows |m\rangle$. Meanwhile, the classical drivings are largely detuned with the transitions $|g\rangle \leftrightarrows |d\rangle$ and $|g\rangle \leftrightarrows |m\rangle$. As a result, in Eq. (3), we do not consider interaction terms between $|g\rangle$ and $|d\rangle/|m\rangle$. In Eq. (4), there is no interaction between the intermediate states and the excited state. These could be achieved by tuning the quantized field in the cavity to be resonant with the transitions $|g\rangle \leftrightarrows |d\rangle$ and $|g\rangle \leftrightarrows |m\rangle$, while being largely detuned with the transitions $|e\rangle \leftrightarrows |d\rangle$ and $|e\rangle \leftrightarrows |m\rangle$.

Assuming the periodical boundary condition, by Fourier transformation, i.e., $a_j^\dagger = \sum_k a_k^\dagger \exp(ikj)/\sqrt{N}$, and with respect to the rotating frame $U_R = \exp(-i\omega_e t|e\rangle\langle e|)$, the total Hamiltonian (1) can be rewritten as

$$H' = \sum_k \omega_k a_k^\dagger a_k + \frac{1}{\sqrt{N}} \left[\sum_k g_1(a_k^\dagger|g\rangle\langle d| + a_k|d\rangle\langle g|) \right. \\ \left. + \sum_k g_2(a_k^\dagger|g\rangle\langle m| + a_k|m\rangle\langle g|) \right] + H_B', \tag{5}$$

$$H_B' = \Delta_e|e\rangle\langle e| + \Omega_d|d\rangle\langle d| + \Omega_m|m\rangle\langle m| + \Omega_p|e\rangle\langle d| \\ + \Omega_c|e\rangle\langle m| + \text{H.c.}, \tag{6}$$

where $\omega_k = \omega_0 - 2\xi\cos(k)$ and $\Delta_e = \Omega_e - \omega_e$. Because the energy levels d and m are metastable, we only consider that there is dissipation on the energy level d. By introducing an imaginary part on the energy of $|d\rangle$, i.e., $\Omega_d = \Omega_d' - i\kappa/2$, with κ being the dissipation rate, we can investigate the effects of the dissipation. This approach is theoretically sound as long as the characteristic frequency of the Hamiltonian is larger than the dissipation rate. By numerical simulations, we

compare the results by the non-Hermitian Hamiltonian approach and the Lindblad-form quantum master equation, which are not shown here. We find that the non-Hermitian Hamiltonian approach faithfully reproduces the key characteristics of the Lindblad-form quantum master equation approach, although it may overestimate the decoherence. Here, the three energy levels d, e, and m constitute the Λ configuration for the EIT. As shown in Appendix A, we can diagonalize Hamiltonian (6) as

$$H'_B = E_1|E_1\rangle\langle E_1| + E_2|E_2\rangle\langle E_2| + E_3|E_3\rangle\langle E_3|, \quad (7)$$

$$|E_i\rangle = \frac{1}{N_i}\Big\{\big[(E_i - \Omega_d - \omega_1)(E_i - \Omega_d - \omega_2) - \Omega_c^2\big]|d\rangle$$
$$+ \Omega_p(E_i - \Omega_d - \omega_2)|e\rangle + \Omega_p\Omega_c|m\rangle\Big\}, \quad (8)$$

where $|E_i\rangle$'s are the eigenstates with eigenenergies $E_i's$, $\omega_1 = \Delta_e - \Omega_d$, and $\omega_2 = \Omega_m - \Omega_d$. The normalization N_i constants are given by

$$N_i^2 = \big|(E_i - \Omega_d - \omega_1)(E_i - \Omega_d - \omega_2) - \Omega_c^2\big|^2$$
$$+ |\Omega_p(E_i - \Omega_d - \omega_2)|^2 + |\Omega_p\Omega_c|^2. \quad (9)$$

By tuning g_1 and g_2 to satisfy $g_1/g_2 = -\Omega_c/\Omega_p$, we have $|E_1\rangle = (g_1|d\rangle + g_2|m\rangle)/g$, with $g = \sqrt{g_1^2 + g_2^2}$ according to Eq. (8). The eigenvalues of the Hamiltonian are

$$E_1 \simeq \frac{\Omega_p^2}{\Omega^2}\Omega_m + \left(1 - \frac{\Omega_p^2}{\Omega^2}\right)\Omega'_d - i\frac{\Omega_c^2}{2\Omega^2}\kappa, \quad (10)$$

$$E_2 \simeq \Omega + \Omega' - i\frac{\Omega_p^2}{4\Omega^2}\kappa, \quad (11)$$

$$E_3 \simeq -\Omega + \Omega' - i\frac{\Omega_p^2}{4\Omega^2}\kappa, \quad (12)$$

where $\Omega^2 = \Omega_c^2 + \Omega_p^2$ and $\Omega' = \Delta_e + \Omega_c^2\Omega_m/\Omega^2 + (1 - \Omega_c^2/\Omega^2)\Omega'_d$. We can see that when $\Omega_c \ll \Omega_p$, the dissipation rate of $|E_1\rangle$ is much smaller than the dissipation rates of $|E_2\rangle$ and $|E_3\rangle$. Therefore, $|E_1\rangle$ is the dark state. In the bases $|E_j\rangle$ ($j = 1, 2, 3$), Hamiltonian (5) can be simplified as

$$H_{\text{eff}} = E_1|E_1\rangle\langle E_1| + \sum_k(\omega_k a_k^\dagger a_k + Ja_k^\dagger|g\rangle\langle E_1| + \text{H.c.}), \quad (13)$$

where $J = g/\sqrt{N}$. Notice that $|E_2\rangle$ and $|E_3\rangle$ are decoupled with the coupled cavities. In other words, we obtain a hybrid system of a two-level atom and a coupled-cavity array. In this two-level atom, the excited state is the weakly dissipative state $|E_1\rangle$, while $|E_2\rangle$ and $|E_3\rangle$ do not interact with the cavity.

In our scheme for QB, we initially inject a photon into one of the cavities. Due to the coupling between the cavities, the photon will transfer between the cavities in the array. When the photon jumps the cavity where the QB is located, the QB will be charged by the photon because of the interaction between the cavity array and the QB. Since the total number of excitations is conserved due to Eq. (13), in the single-excitation subspace, the wave function at time t reads $|\psi(t)\rangle = u(t)|0, E_1\rangle + \sum_k \beta_k(t)a_k^\dagger|0, g\rangle$, where $|0\rangle$ is the vacuum state of the coupled-cavity array the initial condition is $u(0) = 0$, and $\beta_k(0) = 1/\sqrt{N}$. Here, $u(t)$ is the probability

amplitude of the cavities in the vacuum while the atom is in the dark state, and $\beta_k(t)$ is the probability amplitude of the state where there is a photon in the kth cavity mode while the atom is in the ground state. By the Schrödinger equation, we can obtain

$$i\dot{u} = E_1 u + J\sum_k \beta_k, \quad (14)$$

$$i\dot{\beta_k} = \omega_k\beta_k + Ju. \quad (15)$$

Equations ((14) reveal that because of the interaction between the atom and the cavity, the energy of the photon can be transferred to the QB. Applying the Laplace transformation to Eqs. (14) and (15) yields

$$\tilde{u}(p) = \frac{J}{\sqrt{N}}\frac{\sum_k \frac{1}{ip - \omega_k}}{p + iE_1 + \sum_k \frac{J^2}{p + i\omega_k}}. \quad (16)$$

Although Eqs. (14) and (15) can only be solved numerically, we can find approximate solution in the long-time limit by using the inverse Laplace transform on Eq. (16). The singularities of Eq. (16) are determined by

$$p + iE_1 + \sum_k \frac{J^2}{p + i\omega_k} = 0. \quad (17)$$

Here, the branch cuts are defined by $p + i\omega_k = 0$, with $p \in [ip_m, ip_M]$, where $p_m = -\omega_0 - 2\xi$ and $p_M = -\omega_0 + 2\xi$ are respectively the lowest and highest energy of the energy band of the coupled cavities. If $p \notin [-i(\omega_0 + 2\xi), -i(\omega_0 - 2\xi)]$, we can obtain

$$p + iE_1 + \frac{N}{2\pi\xi}\oint_{|z|=1} dz\frac{J^2}{z^2 + Mz + 1} = 0, \quad (18)$$

where $M = (ip - \omega_0)/\xi$. When $ip > \omega_0 + 2\xi$, i.e., $M > 2$, the solution is denoted as p_1, while for $ip < \omega_0 - 2\xi$, i.e., $M < -2$, the solution is denoted as p_2. The detailed calculation is shown in Appendix B.

It is worth noticing that the solutions of Eq. (18) are the eigenenergy of Hamiltonian (13). By Schrödinger equation $H|\Phi\rangle = E|\Phi\rangle$, we can obtain

$$E_1 + \sum_k \frac{J^2}{E - \omega_k} = E. \quad (19)$$

Let us define $E = ip$. Obviously, Eqs. (17) and (19) are equivalent. Since Eq. (18) determines the eigenenergies of the hybrid system, it governs the dynamical evolution of the QB. In other words, it is the spectral characteristics of the whole system that determine the dynamics of the QB. At the same time, we know that the branch cut with $p \in [ip_m, ip_M]$ corresponds to an energy band, while p_1 and p_2 correspond to the two bound states. By substituting the branch cut and the two singularities of Eq. (18) into the inverse Laplace transformation $u(t) = \int_{\sigma-i\infty}^{\sigma+i\infty} dp\tilde{u}(p)e^{pt}/2\pi i$ of Eq. (16), we have

$$u(t) = B_1 Q(p_1)e^{p_1 t} + B_2 Q(p_2)e^{p_2 t} + \int_{-2\xi}^{2\xi} C(x)e^{i(x-\omega_0)t}dx, \quad (20)$$

where

$$Q(p_1) = \frac{g}{\xi\sqrt{M^2 - 4}} = -Q(p_2), \qquad (21)$$

$$B_j = \frac{(ip_j - \omega_0)^2 - 4\xi^2}{(ip_j - \omega_0)^2 - 4\xi^2 + (ip_j - E_1)(ip_j - \omega_0)}, \quad (22)$$

$$C(x) = -\frac{1}{\pi} \frac{\frac{g}{\sqrt{4\xi^2 - (x)^2}}[(x - \omega_0) + E_1]}{(E_1 - \omega_0 + x)^2 + \frac{J^2 N^2}{4\xi^2 - (x)^2}} e^{i(x - \omega_0)t}. \quad (23)$$

Because the energy band $p \in [ip_m, ip_M]$ of the system leads to the occurrence of the branch cut, the contribution of the branch cut tends to zero for a long time due to out-of-phase interference [66,67]. We can obtain the probability $P_{E_1} = |u(\infty)|^2$ in the long-time limit as

$$P_{E_1} \equiv Q(p_1)^2 [B_1^2 + B_2^2 - 2B_1B_2\cos(\phi t)], \qquad (24)$$

where $\phi = ip_1 - ip_2$. When the dissipation κ of the system is absent, ϕ is obviously real. As a result, there is coherent energy exchange between the QB and the charger energy as manifested by the Rabi-like oscillation due to the existence of the two bound states. However, when there is only one bound state, $P_{E_1} \equiv Q(p_1)^2 B_1^2$, and thus the Rabi-like oscillations disappear. Because of the second law of thermodynamics, not all of the QB's energy can be converted to work [26]. Thus, in the rotating frame we can use the ergotropy [24,25] to evaluate the amount of extractable work of the QB via

$$\mathcal{W}(t) = \mathrm{Tr}[\rho'_B(t)H'_B] - \mathrm{Tr}[\tilde{\rho}'_B(t)H'_B], \qquad (25)$$

where $\rho'_B(t) = \mathrm{Tr}_c(|\psi'(t)\rangle\langle\psi'(t)|)$ is the reduced density matrix of the QB, and $\tilde{\rho}'_B(t) = \sum_k r_k(t)|\epsilon_k\rangle\langle\epsilon_k|$ is the passive state of the QB. $r_k(t)$'s are the eigenvalues of $\rho'_B(t)$ in descending order, and $|\epsilon_k\rangle$'s are the eigenstates of H'_B corresponding to the eigenvalues ϵ_k in ascending order. The rotating frame is equivalent to the interaction picture, which aims at eliminating the time dependence of the Hamiltonian and thus enables simplification of the calculation and even allows us to obtain the analytical solution. That is because the transformation between the different frames should not modify the results of any physical quantity but simplify the calculation.

During the charging process, the photon is initially injected into the cavity where the atom is located. By carefully tuning the parameters such that $g_1/g_2 = -\Omega_c/\Omega_p$, the dark state and the two bright states are formed, and only the dark state is coupled to the cavity modes, while the bright states become decoupled. Consequently, the photon interacts selectively with the dark state $|E_1\rangle$, enabling coherent energy transfer from the cavity array to the QB, due to the nature of the EIT.

III. NUMERICAL SIMULATION AND DISCUSSION

In our scheme, the energy is stored in the composite system of the QB and the charger as shown by the Rabi-like oscillations in Eq. (24). This implies that the number of the bound states in the open quantum system is important. Therefore, in Fig. 2, we demonstrate the energy of the bound states and the energy band $\omega_k = \omega_0 - 2\xi\cos(k)$ of the total system. It is shown that when the energy E_1 of the QB is within the energy band, there are two bound states. However, when E_1 is outside of the energy band, only one bound state is present. In other
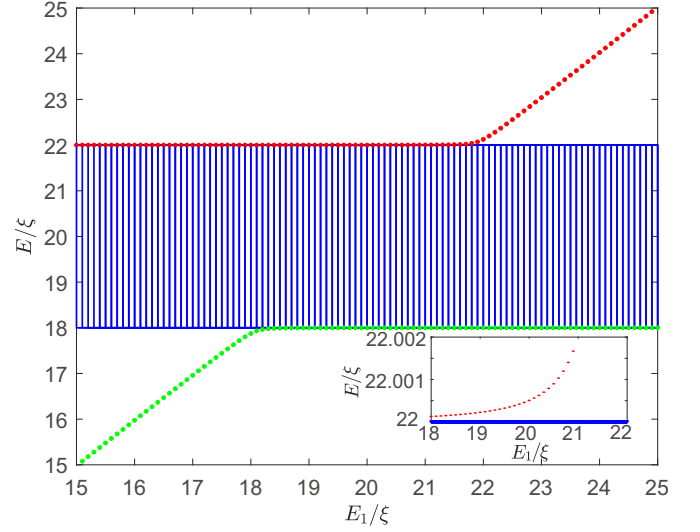

FIG. 2. The dependence of the energy of the bound states on the energy band and the energy E_1 of the QB. The blue solid line is the energy band $\omega_k = \omega_0 - 2\xi\cos(k)$ of the coupled-cavity array. The energies of the bound states denoted by the red and green dots are obtained by Eq. (19). The parameters used in the calculation are $\omega_0 = 20\xi$ and $g = 0.3\xi$.

words, we can effectively modify the number of the bound state in the composite system by tuning the energy of the QB.

In Fig. 3 we investigate the effects of the number of the bound states in the composite system on the probability of the dark state of the QB. Therein, we compare the analytical solutions by Eq. (24) and the numerical simulations. It is shown that the analytical solution coincides with the numerical simulation except for the short-time regime, since we neglect the contribution from the branch cut. In addition to the coherent oscillations, the probability decays due to the dissipation of the QB. Similarly, we also compare the analytical solution and the numerical simulation with the Lindblad-form quantum master equation method [68]. We show that our results are in good agreement with those by the quantum master equation. In Fig. 3(a), we observe a significant Rabi-like coherent oscillation between the atoms and the cavity array. This oscillation reflects the formation of two bound states in the system of atom-cavity-array; i.e., the energy is repeatedly exchanged between the atom and the local cavities without propagating to the cavities far away from the atom. As a result, the energy is localized in the vicinity of the atom, creating an effective "protection zone" that significantly inhibits energy losses to the cavity array. On the contrary, when the energy of the dark state of the QB is outside of the energy band in Fig. 3(b), we find that the probability of the QB being in the dark state is very low, and the oscillation over time is irregular, which is bad for the storage of energy.

In realistic systems, due to the couplings to the environment, there would exist quantum decoherence. In Fig. 4, we plot the envelope of the probability of which the atom is in the dark state in order to explore the effects of the bound states on the energy storage. At the very beginning, the envelope changes somewhat chaotically, which is not shown here. However, after some time it tends to decay exponentially. By
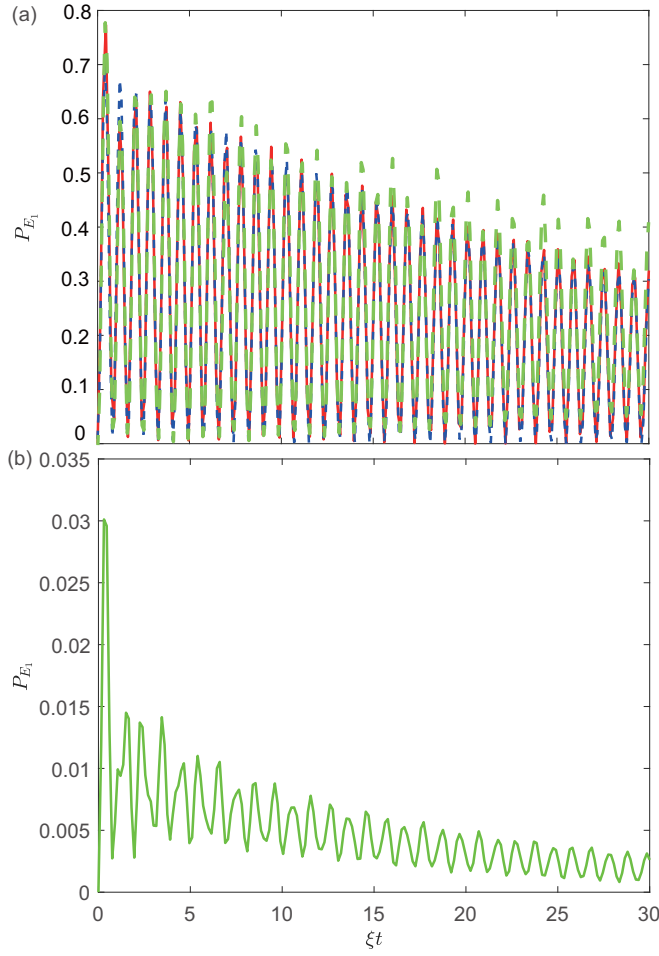
FIG. 3. Probability of the dark state $|E_1\rangle$ vs time t. (a) When E_1 is in the energy band of the coupled cavities, the analytical results obtained by Eq. (24) are denoted as the blue dots, while the numerical results are denoted by the red solid line. In addition, the green dashed line is calculated using the Lindblad-form quantum master equation. The parameters are as follows: $E_1/\xi = 35.327 - 0.032i$, $\omega_0 = 100\xi/3$, $\Omega_d = 106\xi/3$, $\Omega_e = 50\xi$, $\Omega_m = 106\xi/3$, $\kappa = 20\xi/3$, $\Omega_p = 50\xi/3$, $\Omega_c = 5\xi/3$, and the number of cavities $N = 253$. (b) When E_1 is outside of the energy band of the coupled cavities, the numerical results denoted by the green solid line are obtained by $E_1/\xi = 66.6553 - 0.0287i$, $\omega_0 = 100\xi/3$, $\Omega_d = 200\xi/3$, $\Omega_e = 100\xi$, $\Omega_m = 200\xi/3$, $\kappa = 20\xi/3$, $\Omega_p = 50\xi/3$, $\Omega_c = 5\xi/3$, and $N = 253$.

numerical fitting as shown by the red dashed line, we obtain an effective decay rate of $\kappa' = 2.6487 \times 10^{-2}\xi \ll \kappa = 20\xi/3$ when there are two bound states. If we neglect the effect of the cavity array, i.e., exclude the contribution from the bound states, the decay rate of $P_{E_1}(t)$ is given by γ. By numerical fitting as shown by the blue solid line, we obtain the decay rate $\gamma = 0.0645\xi \approx 2\kappa'$. It can be seen that, thanks to the presence of the bound states, the decay rate is further reduced as compared to the case when only the EIT is present. Also, this implies that due to the EIT and the bound states, the dissipation has been significantly inhibited and thus suppresses the degradation of the QB.

Another important physical parameter to assess the QB is the extractable energy, i.e., the ergotropy [25,26] in Eq. (25).
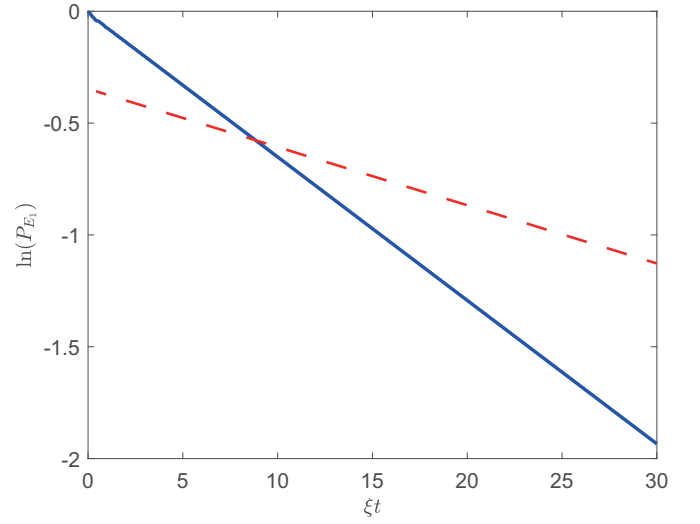

FIG. 4. The envelope of the probability of the dark state with/without two bound states vs time. The red dashed line denotes the case when there are two bound states. We use the function $\ln(P_{E_1}) = -0.35309 - 2.6487 \times 10^{-2}\xi t$ to fit the data with the linear correlation coefficient $|r| = 0.99314$. The blue solid line shows the case when there is no bound state with the corresponding linear correlation coefficient $|r| = 1.0000$. Initially, the atom is in the state $|m\rangle$. The parameters are as follows: $E_1/\xi = 35.327 - 0.032i$, $\Omega_d = 106\xi/3$, $\Omega_e = 50\xi$, $\Omega_m = 106\xi/3$, $\kappa = 20\xi/3$, $\Omega_p = 50\xi/3$, and $\Omega_c = 5\xi/3$.

Since the coupled-cavity array acts as a QB charger, we investigate the relationship between its ability to charge the QB and the parameters. Here, we initially inject the photon into the adjacent cavity of the $0th$ cavity and explore the dynamics of the charging of the QB. The relationship between the ergotropy $\mathcal{W}$ and the frequency ω_0 of the cavity and the coupling strength ξ between two cavities is shown in Fig. 5. For the present set of parameters, we find that, no matter how
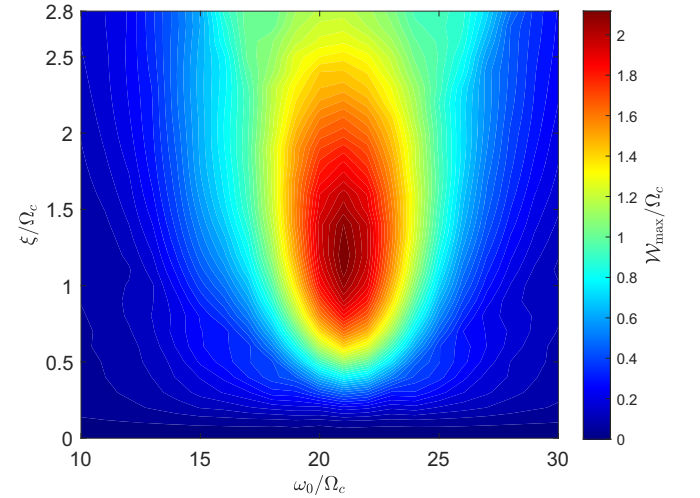

FIG. 5. The maximum ergotropy $\mathcal{W}_{\max}$ during the duration $[0, t_{\max} = 15/\Omega_c]$ vs the coupling strength ξ and the frequency ω_0 of the cavity. The other parameters are $\Omega_d = 21.2\Omega_c$, $\Omega_e = 30\Omega_c$, $\Omega_m = 21.2\Omega_c$, $\kappa = 4\Omega_c$, $\Omega_p = 10\Omega_c$, and $N = 253$.
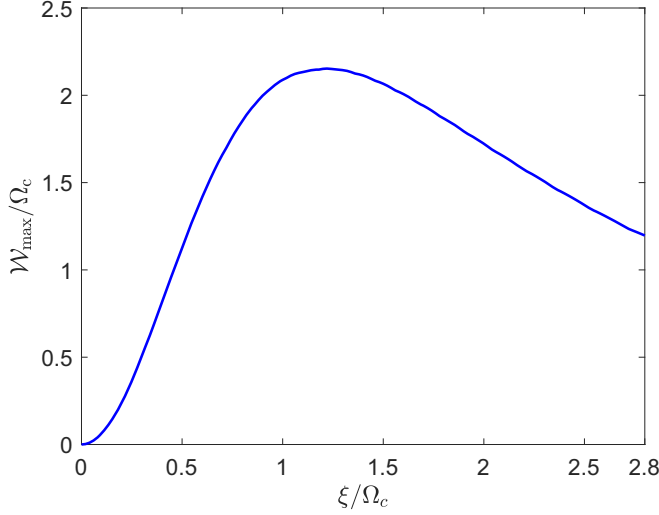
FIG. 6. The dependence of the maximum ergotropy $\mathcal{W}_{\max}$ in the period $[0, t_{\max} = 15/\Omega_c]$ on the coupling between two cavities ξ when $\omega_0 = \mathrm{Re}(E_1)$. The other parameters are as follows: $\omega_0 = 21.196\Omega_c$, $\Omega_d = 21.2\Omega_c$, $\Omega_e = 30\Omega_c$, $\Omega_m = 21.2\Omega_c$, $\kappa = 2\Omega_c$, $\Omega_p = 10\Omega_c$, and $N = 253$.
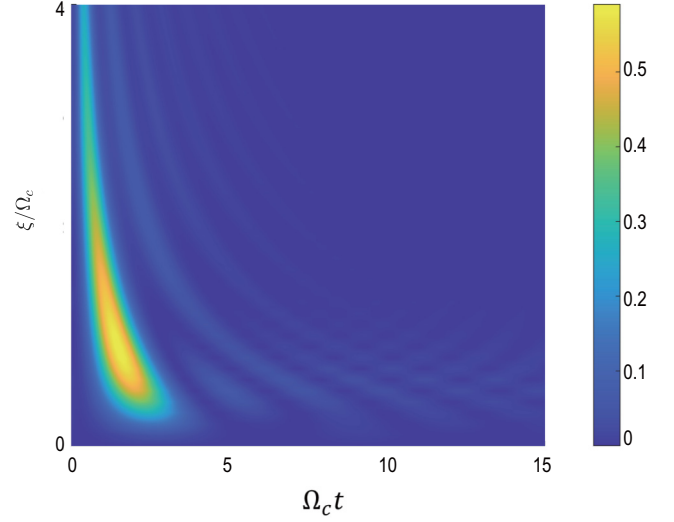

FIG. 7. The average charging power P/Ω_c^2 as a function of the coupling strength ξ and time. The parameters are $\omega_0 = 21.196\Omega_c$, $\Omega_d = 21.2\Omega_c$, $\Omega_e = 30\Omega_c$, $\Omega_m = 21.2\Omega_c$, $\kappa = 4\Omega_c$, $\Omega_p = 10\Omega_c$, and $N = 253$.

ξ changes, there is a maximum value of $\mathcal{W}$ when ω_0 is equal to the energy E_1 of the dark state. This implies that both the useful work and the efficiency of the QB are the largest when the cavity and the QB are in resonance. In Fig. 6, we explore the relation between the maximum ergotropy $\mathcal{W}_{\max}$ of the QB and the coupling strength ξ under the resonance condition with $E_1 = (21.196 - 0.019i)\Omega_c$. We find that for small ξ, $\mathcal{W}_{\max}$ increases along with the rise of ξ, because the coupling between the cavities helps deliver the photon to the cavity where the atom is located. However, after it reaches the maximum around $\xi = 1.22\Omega_c$, $\mathcal{W}_{\max}$ experiences a decrease when further increasing the coupling strength. This suggests that strong coupling between the cavities can prompt the delivered photon away from the cavity with the atom and thus suppresses the ergotropy. In summary, the coupling between the two cavities can improve the efficiency of the QB assisted by the resonance between the QB and the cavity.

Finally, we discuss the effects of the charging time and the coupling strength ξ on the average charging power, which is defined as $P(t) = W(t)/t$ [43]. The average charging power is critical for QBs as it helps determine the optimal time to turn off the charging. When the average charging power is high, it indicates that the QB is charging rapidly. On the contrary, when the average charging power is low, it suggests that the change in the QB's ergotropy is slow. As shown in Fig. 7, we can observe that, for a given coupling strength ξ, the charging power increases quickly and then decreases, eventually stabilizing at a relatively low steady state. By varying ξ, we find that there is an optimal value of ξ for maximizing the average charging power. A larger ξ does not necessarily lead to better performance in the average charging power, and this insight can guide us in optimizing the QB in experiments.

In the above analysis of the effects of the photon frequency ω_0 and the coupling strength ξ on the ergotropy and the

average charging power of the QB, our purpose is to identify the optimal experimental parameters. The QB can be optimized in advance according to the requirements of the load, thereby fixing its parameters. During the charging or discharging processes, these parameters remain unchanged.

IV. CONCLUSION

In this paper, we propose a scheme for charging QB by coupling QB with cavity array. With the EIT, we obtain the QB of an effective two-level system including the dark state and the ground state. When the energy of the dark state is within the energy band of the cavity array, there are two bound states. We show that the energies of the bound states determine the distribution dynamics of QB in the excited state, resulting in Rabi-like oscillations. Under the influence of the bound states and the dark state, we find that the dissipation of the environment is strongly suppressed. When the energy of the dark state is resonant with the bare frequency of the cavity, the extractable work of the QB reaches its maximum. In addition, we demonstrate that the coupling strength of the two cavities maximizes the extractable work of the QB. Our scheme extends the QB's lifetime and avoids the reduction in charging efficiency by suppressing environmental decoherence, providing an avenue for efficient QB charging.

The data that support the findings of this article are not publicly available. The data are available from the authors upon reasonable request.

APPENDIX A: DIAGONALIZATION OF ATOMIC HAMILTONIAN

In this section, we obtain the eigenvalues and eigenstates of atomic Hamiltonian by the perturbation theory.

After the Fourier transformation, the total Hamiltonian is given by

$$
H = \sum_k \omega_k a_k^\dagger a_k + \frac{1}{\sqrt{N}} \sum_k g_1(a_k^\dagger |g\rangle\langle d| + a_k |d\rangle\langle g|)
$$
$$
+ \frac{1}{\sqrt{N}} \sum_k g_2(a_k^\dagger |g\rangle\langle m| + a_k |m\rangle\langle g|) + H_0, \quad \text{(A1)}
$$

where

$$
H_B = \Omega_d |d\rangle\langle d| + \Omega_e |e\rangle\langle e| + \Omega_m |m\rangle\langle m|
$$
$$
+ \Omega_p e^{-i\omega_p t} |e\rangle\langle d| + \Omega_c e^{-i\omega_c t} |e\rangle\langle m| + \text{H.c.}, \quad \text{(A2)}
$$

with $\omega_k = \omega_0 - 2\xi \cos(k)$ and $\Omega_d = \Omega_d' - i\kappa/2$. In the rotating frame defined by $U_R = \exp(-i\omega_e t |e\rangle\langle e|)$, the Hamiltonian (A2) is rewritten as

$$
H_B' = U_R^\dagger H_0 U_R - iU_R^\dagger \dot{U}_R
$$
$$
= \Omega_d |d\rangle\langle d| + (\Omega_e - \omega_e)|e\rangle\langle e| + \Omega_m |m\rangle\langle m|
$$
$$
+ \Omega_p e^{-i(\omega_p - \omega_e)t} |e\rangle\langle d| + \Omega_c e^{-i(\omega_c - \omega_e)t} |e\rangle\langle m| + \text{H.c.}
$$
$$
\text{(A3)}
$$

Assuming $\omega_p = \omega_e = \omega_c$, we obtain

$$
H_B' = \Delta_e |e\rangle\langle e| + \Omega_d |d\rangle\langle d| + \Omega_m |m\rangle\langle m|
$$
$$
+ \Omega_p |e\rangle\langle d| + \Omega_c |e\rangle\langle m| + \text{H.c.}, \quad \text{(A4)}
$$

with $\Delta_e = \Omega_e - \omega_e$. Defining $E = y + \Omega_d$, the eigenvalue E of Hamiltonian (A4) is determined by

$$
\begin{vmatrix} -y & \Omega_p & \\ \Omega_p & \omega_1 - y & \Omega_c \\ & \Omega_c & \omega_2 - y \end{vmatrix} = 0, \quad \text{(A5)}
$$

with $\omega_1 = \Delta_e - \Omega_d$ and $\omega_2 = \Omega_m - \Omega_d$, which is equivalent to

$$
y^3 - y^2(\omega_1 + \omega_2) + y(\omega_1\omega_2 - \Omega_c^2 - \Omega_p^2) = -\Omega_p^2\omega_2. \quad \text{(A6)}
$$

If we assume ω_2 is small, to the first order of ω_2, the solutions can be written as $y_j = y_{0j} + A_j\omega_2$ ($j = 1, 2, 3$). By the perturbation theory, we can approximate Eq. (A6) to the zeroth order as

$$
y^3 - y^2(\omega_1 + \omega_2) + y(\omega_1\omega_2 - \Omega_c^2 - \Omega_p^2) = 0. \quad \text{(A7)}
$$

Thus, we can obtain

$$
y_{01} = 0, \quad \text{(A8)}
$$

$$
y_{02} = \omega_+, \quad \text{(A9)}
$$

$$
y_{03} = \omega_-, \quad \text{(A10)}
$$

with $\Omega^2 = \Omega_c^2 + \Omega_p^2$ and $\omega_\pm = [(\omega_1 + \omega_2) \pm \sqrt{(\omega_1 - \omega_2)^2 + 4\Omega^2}]/2$. If $\omega_1, \omega_2 \ll \Omega$, we can approximate $\omega_\pm$ as

$$
\omega_\pm \simeq \frac{1}{2}\left\{\omega_1 + \omega_2 \pm 2\Omega\left[1 + \frac{(\omega_1 - \omega_2)^2}{4\Omega^2}\right]\right\}
$$
$$
\simeq \frac{1}{2}[\omega_1 + \omega_2 \pm 2\Omega]. \quad \text{(A11)}
$$

Substituting the zeroth-order solutions y_{0j} into Eq. (A6) yields

$$
A_1 = -\frac{\Omega_p^2}{\omega_+\omega_-}, \quad \text{(A12)}
$$

$$
A_2 = -\frac{\Omega_p^2}{\omega_+(\omega_+ - \omega_-)}, \quad \text{(A13)}
$$

$$
A_3 = \frac{\Omega_p^2}{\omega_-(\omega_+ - \omega_-)}. \quad \text{(A14)}
$$

In conclusion, we could obtain the eigenvalues of Hamiltonian H_0' as

$$
E_1 = -\frac{\Omega_p^2}{1/4 * [(\omega_1 + \omega_2)^2 - 4\Omega^2]}\omega_2 + \Omega_d
$$
$$
\simeq \frac{\Omega_p^2}{\Omega^2}\omega_2 + \Omega_d, \quad \text{(A15)}
$$

$$
E_2 = \frac{1}{2}[\omega_1 + \omega_2 + 2\Omega] - \frac{\Omega_p^2}{\omega_+(\omega_+ - \omega_-)}\omega_2
$$
$$
\simeq \Omega + \frac{1}{2}\left(\omega_1 + \frac{\Omega_c^2}{\Omega^2}\omega_2\right) + \Omega_d, \quad \text{(A16)}
$$

$$
E_3 = \frac{1}{2}[\omega_1 + \omega_2 - 2\Omega] + \frac{\Omega_p^2}{\omega_+(\omega_+ - \omega_-)}\omega_2
$$
$$
\simeq -\Omega + \frac{1}{2}\left(\omega_1 + \frac{\Omega_c^2}{\Omega^2}\omega_2\right) + \Omega_d. \quad \text{(A17)}
$$

Correspondingly, the eigenstates are respectively

$$
|E_i\rangle = \frac{1}{N_i}\left\{[(E_i - \Omega_d - \omega_1)(E_i - \Omega_d - \omega_2) - \Omega_c^2]|d\rangle \right.
$$
$$
\left. + \Omega_p(E_i - \Omega_d - \omega_2)|e\rangle + \Omega_p\Omega_c|m\rangle\right\}, \quad \text{(A18)}
$$

where the normalization constants are given by

$$
N_i^2 = |(E_i - \Omega_d - \omega_1)(E_i - \Omega_d - \omega_2) - \Omega_c^2|^2
$$
$$
+ |\Omega_p(E_i - \Omega_d - \omega_2)|^2 + |\Omega_p\Omega_c|^2. \quad \text{(A19)}
$$

To the zeroth order of ω_j's, we can simplify the eigenstates as

$$
|E_1\rangle = \frac{1}{N_1}\left(-\Omega_c^2|d\rangle + \Omega_p\Omega_c|m\rangle\right), \quad \text{(A20)}
$$

$$
|E_2\rangle = \frac{1}{N_2}\left(\Omega_p^2|d\rangle + \Omega_p\Omega|e\rangle + \Omega_p\Omega_c|m\rangle\right), \quad \text{(A21)}
$$

$$
|E_3\rangle = \frac{1}{N_3}\left(\Omega_p^2|d\rangle - \Omega_p\Omega|e\rangle + \Omega_p\Omega_c|m\rangle\right), \quad \text{(A22)}
$$

with $N_1 = \Omega\Omega_c$, $N_2 = \sqrt{2}\Omega\Omega_p$, and $N_3 = \sqrt{2}\Omega\Omega_p$. Here, $|E_1\rangle$ is the dark state, while $|E_2\rangle$ and $|E_3\rangle$ are the bright states.

Furthermore, the bare atomic states can rewritten in terms of the eigenstates as

$$|d\rangle = \frac{1}{2\Omega^2}(N_2|E_2\rangle + N_3|E_3\rangle - 2N_1|E_1\rangle), \quad \text{(A23)}$$

$$|e\rangle = \frac{1}{2\Omega_p\Omega}(N_2|E_2\rangle - N_3|E_3\rangle), \quad \text{(A24)}$$

$$|m\rangle = \frac{1}{2\Omega_p\Omega_c}(N_2|E_2\rangle + N_3|E_3\rangle + 2N_1|E_1\rangle). \quad \text{(A25)}$$

APPENDIX B: EVOLUTION OF THE DARK STATE

In the rotating frame defined by $U_R = \exp(-i\omega_e t|e\rangle\langle e|)$, the Hamiltonian of the hybrid system including the four-level atoms and the cavity array can be transformed as

$$H' = \sum_k \omega_k a_k^\dagger a_k + \frac{1}{\sqrt{N}}\Bigg[\sum_k g_1(a_k^\dagger|g\rangle\langle d| + a_k|d\rangle\langle g|)$$
$$+ \sum_k g_2(a_k^\dagger|g\rangle\langle m| + a_k|m\rangle\langle g|)\Bigg] + H_0'. \quad \text{(B1)}$$

Assuming $g_1/g_2 = -\Omega_c/\Omega_p$, we can obtain $|E_1\rangle = (g_1|d\rangle + g_2|m\rangle)/g$, with $g = \sqrt{g_1^2 + g_2^2}$. In the bases $|E_1\rangle$ ($j = 1, 2, 3$), Hamiltonian (B1) can be simplified as

$$H_{\text{eff}} = \sum_k \omega_k a_k^\dagger a_k + E_1|E_1\rangle\langle E_1|$$
$$+ J\sum_k(a_k^\dagger|g\rangle\langle E_1| + a_k|E_1\rangle\langle g|), \quad \text{(B2)}$$

with $J = g/\sqrt{N}$. Note that the bright states $|E_2\rangle$ and $|E_3\rangle$ are decoupled from the cavity modes in Eq. (B2). In the single-excitation subspace, the state of the total system reads

$$|\psi(t)\rangle = u(t)|0, E_1\rangle + \sum_k \beta_k(t)a_k^\dagger|0, g\rangle. \quad \text{(B3)}$$

Here, $|0, E_1\rangle$ is the cavities in the vacuum while the atom is in the dark state. $a_k^\dagger|0, g\rangle$ is the state where there is a photon in the kth cavity mode while the atom is in the ground state. Using the Schrödinger equation for Eqs. (B2) and (B3), we can obtain

$$i\dot{u} = E_1 u + J\sum_k \beta_k, \quad \text{(B4)}$$

$$i\dot{\beta}_k = \omega_k\beta_k + Ju, \quad \text{(B5)}$$

where $u(0) = 0$ and $\beta_k(0) = 1/\sqrt{N}$ are the initial conditions of the system. Next, we apply a Laplace transformation to Eqs. (B4) and (B5) to obtain

$$i[p\tilde{u}(p) - u(0)] = E_1\tilde{u}(p) + J\sum_k \tilde{\beta}_k(p), \quad \text{(B6)}$$

$$i[p\tilde{\beta}_k(p) - \beta_k(0)] = \omega_k\tilde{\beta}_k(p) + J\tilde{u}(p). \quad \text{(B7)}$$

With a bit of algebra, we can calculate the probability amplitude of $|0, E_1\rangle$ in p space as follows:

$$\tilde{u}(p) = \frac{J}{\sqrt{N}}\frac{\sum_k \frac{1}{ip-\omega_k}}{p + iE_1 + \sum_k \frac{J^2}{p+i\omega_k}}. \quad \text{(B8)}$$

The probability amplitude of $|0, E_1\rangle$ in the time domain can be obtained from the inverse Laplace transform as

$$u(t) = \frac{1}{2\pi i}\int_{\sigma-i\infty}^{\sigma+i\infty} dp\,\tilde{u}(p)e^{pt}$$
$$= \sum_j \text{res}[\tilde{u}(p_j)e^{p_j t}] - \frac{1}{2\pi i}\Bigg[\int_{C_R} dp\,\tilde{u}(p)e^{pt}$$
$$+ \int_{l_1} dp\,\tilde{u}(p)e^{pt} + \int_{l_2} dp\,\tilde{u}(p)e^{pt}\Bigg]. \quad \text{(B9)}$$

Here, C_R is the large semicircle in infinity, p_j's and l_j's ($j = 1, 2$) are the two singularities and the two branch cuts, respectively, which are defined from

$$p + iE_1 + \sum_k \frac{J^2}{p+i\omega_k} = 0. \quad \text{(B10)}$$

Following Eq. (B10), the branch cuts are defined by $p + i\omega_k = 0$, with $p \in [ip_m, ip_M]$, where $p_m = -\omega_0 - 2\xi$ and $p_M = -\omega_0 + 2\xi$. Please note

$$\sum_k \frac{1}{p+i\omega_k} = \frac{N}{2\pi}\int dk\frac{1}{p + i[\omega_0 - 2\xi\cos(k)]}$$
$$= \frac{N}{2\pi}\int_{-\pi}^{\pi} dk\frac{1}{p + i[\omega_0 - \xi(e^{ik} + e^{-ik})]}$$
$$= \frac{N}{2\pi}\oint_{|z|=1} dz\frac{1}{p + i[\omega_0 - \xi(z + z^{-1})]}\frac{1}{iz}$$
$$= \frac{N}{2\pi\xi}\oint_{|z|=1} dz\frac{1}{z^2 + \frac{(ip-\omega_0)z}{\xi} + 1}$$
$$= \frac{N}{2\pi\xi}\oint_{|z|=1} dz\frac{1}{z^2 + Mz + 1}, \quad \text{(B11)}$$

where $M = (ip - \omega_0)/\xi$, and $z_\pm = [-M \pm \sqrt{M^2 - 4}]/2$ are the two singularities. Thus, if $p \notin [-i(\omega_0 + 2\xi), -i(\omega_0 - 2\xi)]$, we have $M > 2$ or $M < -2$. For the former case, since $ip > \omega_0 + 2\xi$, i.e., $-1 < z_+ < 0$ and $z_- < -1$, we have

$$\frac{N}{2\pi\xi}\oint_{|z|=1} dz\frac{1}{z^2 + Mz + 1}$$
$$= \frac{N}{2\pi\xi}\oint_{|z|=1} dz\frac{1}{(z - z_+)(z - z_-)}$$
$$= \frac{iN}{\xi\sqrt{M^2 - 4}}. \quad \text{(B12)}$$

In order to obtain the singularity, we substitute Eq. (B12) into Eq. (B10), and thus we have

$$p + iE_1 + J^2\frac{iN}{\xi\sqrt{M^2 - 4}} = f_1(p). \quad \text{(B13)}$$

Letting $f_1(p) = 0$, we can obtain the singularity p_1 with $ip_1 > \omega_0 + 2\xi$. Similarly, for the latter case, we can also obtain the second singularity p_2 with $ip_2 < \omega_0 - 2\xi$ by

$$p + iE_1 - J^2\frac{iN}{\xi\sqrt{M^2 - 4}} = f_2(p). \quad \text{(B14)}$$

In the above calculations, we can obtain the contribution from the singularity in Eq. (B8). Hereafter, we obtain the contribution from the branch cuts in Eq. (B8). Because of the Jordan lemma, we can know $\int_{C_R} dp\,\tilde{u}(p)e^{pt} = 0$. So far as the contribution from the branch cuts, that is, $p \in [ip_m, ip_M]$, we can obtain

$$\int_{l_1} dp\,\tilde{u}(p)e^{pt} + \int_{l_2} dp\,\tilde{u}(p)e^{pt} = \int_{p_m}^{p_M} \frac{-J/\sqrt{N}\sum_k \frac{1}{p+\omega_k+i0^+}e^{ipt}}{p+E_1 - \sum_k \frac{J^2}{p+\omega_k+i0^+}}dp + \int_{p_M}^{p_m} \frac{-J/\sqrt{N}\sum_k \frac{1}{p+\omega_k-i0^+}e^{ipt}}{p+E_1 - \sum_k \frac{J^2}{p+\omega_k-i0^+}}dp. \tag{B15}$$

Here,

$$\sum_k \frac{1}{p+\omega_k \pm i0^+} = \frac{N}{2\pi}\int_{-\pi}^{\pi} dk \frac{1}{p+\omega_k \pm i0^+} = \frac{N}{2\pi}\left[\int_{-\pi}^{\pi} dk\, P\left(\frac{1}{p+\omega_k}\right) \mp \frac{i2\pi}{\sqrt{4\xi^2 - (\omega_0 + p)^2}}\right], \tag{B16}$$

where $P(x)$ is the principal value of x, and $\int_{-\pi}^{\pi} dk\, P[1/(p+\omega_k)] = 0$. Substituting Eq. (B16) into Eq. (B15) yields

$$\int_{p_m}^{p_M} \frac{-\frac{J}{\sqrt{N}}\sum_k \frac{1}{p+\omega_k+i0^+}e^{ipt}}{p+E_1 - \sum_k \frac{J^2}{p+\omega_k+i0^+}}dp + \int_{p_M}^{p_m} \frac{-\frac{J}{\sqrt{N}}\sum_k \frac{1}{p+\omega_k-i0^+}e^{ipt}}{p+E_1 - \sum_k \frac{J^2}{p+\omega_k-i0^+}}dp = \frac{J}{\sqrt{N}}\int_{-2\xi}^{2\xi} \frac{\frac{2iN}{\sqrt{4\xi^2-(x)^2}}[(x-\omega_0)+E_1]}{(E_1-\omega_0+x)^2 + \frac{J^2N^2}{4\xi^2-(x)^2}}e^{i(x-\omega_0)t}dx. \tag{B17}$$

Thus, we can obtain

$$-\frac{1}{2\pi i}\left(\int_{l_1} dp\,\tilde{u}(p)e^{pt} + \int_{l_2} dp\,\tilde{u}(p)e^{pt}\right) = \int_{-2\xi}^{2\xi} C(x)e^{i(x-\omega_0)t}dx, \tag{B18}$$

where

$$C(x) = -\frac{1}{\pi}\frac{\frac{g}{\sqrt{4\xi^2-(x)^2}}[(x-\omega_0)+E_1]}{(E_1-\omega_0+x)^2 + \frac{J^2N^2}{4\xi^2-(x)^2}}e^{i(x-\omega_0)t}. \tag{B19}$$

In summary, we can write the expression of the probability amplitude of $|0, E_1\rangle$ as

$$u(t) = B_1 Q(p_1)e^{p_1 t} + B_2 Q(p_2)e^{p_2 t} + \int_{-2\xi}^{2\xi} C(x)e^{i(x-\omega_0)t}dx, \tag{B20}$$

where

$$Q(p_1) = \frac{g}{\xi\sqrt{M^2-4}}, \tag{B21}$$

$$Q(p_2) = -\frac{g}{\xi\sqrt{M^2-4}}, \tag{B22}$$

$$B_j = \frac{1}{\frac{df_j}{dp}\big|_{p_j}} = \frac{(ip_j-\omega_0)^2 - 4\xi^2}{(ip_j-\omega_0)^2 - 4\xi^2 + (ip_j-E_1)(ip_j-\omega_0)}. \tag{B23}$$

[1] K. Bharti, A. Cervera-Lierta, T. H. Kyaw, T. Haug, S. Alperin-Lea, A. Anand, M. Degroote, H. Heimonen, J. S. Kottmann, T. Menke, W.-K. Mok, S. Sim, L.-C. Kwek, and A. Aspuru-Guzik, Noisy intermediate-scale quantum algorithms, Rev. Mod. Phys. **94**, 015004 (2022).

[2] F. Xu, X. Ma, Q. Zhang, H.-K. Lo, and J.-W. Pan, Secure quantum key distribution with realistic devices, Rev. Mod. Phys. **92**, 025002 (2020).

[3] M. Esposito, U. Harbola, and S. Mukamel, Nonequilibrium fluctuations, fluctuation theorems, and counting statistics in quantum systems, Rev. Mod. Phys. **81**, 1665 (2009).

[4] S. Vinjanampathy and J. Anders, Quantum thermodynamics, Contemp. Phys. **57**, 545 (2016).

[5] G. Benenti, G. Casati, K. Saito, and R. Whitney, Fundamental aspects of steady-state conversion of heat to work at the nanoscale, Phys. Rep. **694**, 1 (2017).

[6] M. Carrega, L. M. Cangemi, G. De Filippis, V. Cataudella, G. Benenti, and M. Sassetti, Engineering dynamical couplings for quantum thermodynamic tasks, PRX Quantum **3**, 010323 (2022).

[7] M. Campisi and J. Goold, Thermodynamics of quantum information scrambling, Phys. Rev. E **95**, 062127 (2017).

[8] J. Goold, M. Huber, A. Riera, L. del Rio, and P. Skrzypczyk, The role of quantum information in thermodynamics—a topical review, J. Phys. A **49**, 143001 (2016).

[9] J. Anders and M. Esposito, Focus on quantum thermodynamics, New J. Phys. **19**, 010201 (2017).

[10] R. Kosloff, Quantum thermodynamics: A dynamical viewpoint, Entropy **15**, 2100 (2013).

[11] M. T. Mitchison, Quantum thermal absorption machines: Refrigerators, engines and clocks, Contemp. Phys. **60**, 164 (2019).

[12] J. Klatzow, J. N. Becker, P. M. Ledingham, C. Weinzetl, K. T. Kaczmarek, D. J. Saunders, J. Nunn, I. A. Walmsley, R. Uzdin, and E. Poem, Experimental demonstration of quantum effects in the operation of microscopic heat engines, Phys. Rev. Lett. **122**, 110601 (2019).

[13] J. Roßnagel, O. Abah, F. Schmidt-Kaler, K. Singer, and E. Lutz, Nanoscale heat engine beyond the Carnot limit, Phys. Rev. Lett. **112**, 030602 (2014).

[14] N. Linden, S. Popescu, and P. Skrzypczyk, How small can thermal machines be? The smallest possible refrigerator, Phys. Rev. Lett. **105**, 130401 (2010).

[15] M. O. Scully, M. S. Zubairy, G. S. Agarwal, and H. Walther, Extracting work from a single heat bath via vanishing quantum coherence, Science **299**, 862 (2003).

[16] R. Alicki and M. Fannes, Entanglement boost for extractable work from ensembles of quantum batteries, Phys. Rev. E **87**, 042123 (2013).

[17] K. V. Hovhannisyan, M. Perarnau-Llobet, M. Huber, and A. Acín, Entanglement generation is not necessary for optimal work extraction, Phys. Rev. Lett. **111**, 240401 (2013).

[18] F. C. Binder, S. Vinjanampathy, K. Modi, and J. Goold, Quantacell: Powerful charging of quantum batteries, New J. Phys. **17**, 075015 (2015).

[19] M. Perarnau-Llobet, K. V. Hovhannisyan, M. Huber, P. Skrzypczyk, N. Brunner, and A. Acín, Extractable work from correlations, Phys. Rev. X **5**, 041011 (2015).

[20] G. M. Andolina, M. Keck, A. Mari, M. Campisi, V. Giovannetti, and M. Polini, Extractable work, the role of correlations, and asymptotic freedom in quantum batteries, Phys. Rev. Lett. **122**, 047702 (2019).

[21] J. Oppenheim, M. Horodecki, P. Horodecki, and R. Horodecki, Thermodynamical approach to quantifying quantum correlations, Phys. Rev. Lett. **89**, 180402 (2002).

[22] J.-Y. Gyhm and U. R. Fischer, Beneficial and detrimental entanglement for quantum battery charging, AVS Quantum Sci. **6**, 012001 (2024).

[23] R. Uzdin, A. Levy, and R. Kosloff, Equivalence of quantum heat machines, and quantum-thermodynamic signatures, Phys. Rev. X **5**, 031044 (2015).

[24] B. Çakmak, Ergotropy from coherences in an open quantum system, Phys. Rev. E **102**, 042111 (2020).

[25] G. Francica, F. C. Binder, G. Guarnieri, M. T. Mitchison, J. Goold, and F. Plastina, Quantum coherence and ergotropy, Phys. Rev. Lett. **125**, 180603 (2020).

[26] J. Monsel, M. Fellous-Asiani, B. Huard, and A. Auffèves, The energetic cost of work extraction, Phys. Rev. Lett. **124**, 130601 (2020).

[27] X. Yang, Y.-H. Yang, M. Alimuddin, R. Salvia, S.-M. Fei, L.-M. Zhao, S. Nimmrichter, and M.-X. Luo, Battery capacity of energy-storing quantum systems, Phys. Rev. Lett. **131**, 030402 (2023).

[28] D. Šafránek, D. Rosa, and F. C. Binder, Work extraction from unknown quantum sources, Phys. Rev. Lett. **130**, 210401 (2023).

[29] H.-L. Shi, S. Ding, Q.-K. Wan, X.-H. Wang, and W.-L. Yang, Entanglement, coherence, and extractable work in quantum batteries, Phys. Rev. Lett. **129**, 130602 (2022).

[30] R. Salvia, M. Perarnau-Llobet, G. Haack, N. Brunner, and S. Nimmrichter, Quantum advantage in charging cavity and spin batteries by repeated interactions, Phys. Rev. Res. **5**, 013155 (2023).

[31] P. Chen, T. S. Yin, Z. Q. Jiang, and G. R. Jin, Quantum enhancement of a single quantum battery by repeated interactions with large spins, Phys. Rev. E **106**, 054119 (2022).

[32] S. Seah, M. Perarnau-Llobet, G. Haack, N. Brunner, and S. Nimmrichter, Quantum speed-up in collisional battery charging, Phys. Rev. Lett. **127**, 100601 (2021).

[33] G. M. Andolina, D. Farina, A. Mari, V. Pellegrini, V. Giovannetti, and M. Polini, Charger-mediated energy transfer in exactly solvable models for quantum batteries, Phys. Rev. B **98**, 205423 (2018).

[34] T. F. F. Santos, Y. V. de Almeida, and M. F. Santos, Vacuum-enhanced charging of a quantum battery, Phys. Rev. A **107**, 032203 (2023).

[35] X. Hao, K. Yan, J. Tan, and Q.-Y. Wu, Quantum work extraction of an accelerated Unruh-Dewitt battery in relativistic motion, Phys. Rev. A **107**, 012207 (2023).

[36] M. B. Arjmandi, A. Shokri, E. Faizi, and H. Mohammadi, Performance of quantum batteries with correlated and uncorrelated chargers, Phys. Rev. A **106**, 062609 (2022).

[37] A. C. Santos, B. Çakmak, S. Campbell, and N. T. Zinner, Stable adiabatic quantum batteries, Phys. Rev. E **100**, 032107 (2019).

[38] J. Joshi and T. S. Mahesh, Experimental investigation of a quantum battery using star-topology NMR spin systems, Phys. Rev. A **106**, 042601 (2022).

[39] R.-H. Zheng, W. Ning, Z.-B. Yang, Y. Xia, and S.-B. Zheng, Demonstration of dynamical control of three-level open systems with a superconducting qutrit, New J. Phys. **24**, 063031 (2022).

[40] C.-K. Hu, J. Qiu, P. J. P. Souza, J. Yuan, Y. Zhou, L. Zhang, J. Chu, X. Pan, L. Hu, J. Li, Y. Xu, Y. Zhong, S. Liu, F. Yan, D. Tan, R. Bachelard, C. J. Villas-Boas, A. C. Santos, and D. Yu, Optimal charging of a superconducting quantum battery, Quantum Sci. Technol. **7**, 045018 (2022).

[41] I. Maillette de Buy Wenniger, S. E. Thomas, M. Maffei, S. C. Wein, M. Pont, N. Belabas, S. Prasad, A. Harouri, A. Lemaître, I. Sagnes, N. Somaschi, A. Auffèves, and P. Senellart, Experimental analysis of energy transfers between a quantum emitter and light fields, Phys. Rev. Lett. **131**, 260401 (2023).

[42] G. Zhu, Y. Chen, Y. Hasegawa, and P. Xue, Charging quantum batteries via indefinite causal order: Theory and experiment, Phys. Rev. Lett. **131**, 240401 (2023).

[43] D. Ferraro, M. Campisi, G. M. Andolina, V. Pellegrini, and M. Polini, High-power collective charging of a solid-state quantum battery, Phys. Rev. Lett. **120**, 117702 (2018).

[44] R. Grazi, D. Sacco Shaikh, M. Sassetti, N. Traverso Ziani, and D. Ferraro, Controlling energy storage crossing quantum phase

transitions in an integrable spin quantum battery, Phys. Rev. Lett. **133**, 197001 (2024).

[45] D. Farina, G. M. Andolina, A. Mari, M. Polini, and V. Giovannetti, Charger-mediated energy transfer for quantum batteries: An open-system approach, Phys. Rev. B **99**, 035421 (2019).

[46] J. Liu, D. Segal, and G. Hanna, Loss-free excitonic quantum battery, J. Phys. Chem. C **123**, 18303 (2019).

[47] F. Pirmoradian and K. Mølmer, Aging of a quantum battery, Phys. Rev. A **100**, 043833 (2019).

[48] Y. Yao and X. Q. Shao, Optimal charging of open spin-chain quantum batteries via homodyne-based feedback control, Phys. Rev. E **106**, 014138 (2022).

[49] S.-Y. Bai and J.-H. An, Floquet engineering to reactivate a dissipative quantum battery, Phys. Rev. A **102**, 060201(R) (2020).

[50] S. E. Harris, J. E. Field, and A. Imamoğlu, Nonlinear optical processes using electromagnetically induced transparency, Phys. Rev. Lett. **64**, 1107 (1990).

[51] J. R. Boon, E. Zekou, D. McGloin, and M. H. Dunn, Comparison of wavelength dependence in cascade-, Λ-, and Vee-type schemes for electromagnetically induced transparency, Phys. Rev. A **59**, 4675 (1999).

[52] Y.-Y. Wang, J. Qiu, Y.-Q. Chu, M. Zhang, J. Cai, Q. Ai, and F.-G. Deng, Dark state polarizing a nuclear spin in the vicinity of a nitrogen-vacancy center, Phys. Rev. A **97**, 042313 (2018).

[53] H. Dong, D.-Z. Xu, J.-F. Huang, and C.-P. Sun, Coherent excitation transfer *via* the dark-state channel in a bionic system, Light Sci. Appl. **1**, e2 (2012).

[54] Y.-D. Wang and A. A. Clerk, Using interference for high fidelity quantum state transfer in optomechanics, Phys. Rev. Lett. **108**, 153603 (2012).

[55] B. Khanaliloo, H. Jayakumar, A. C. Hryciw, D. P. Lake, H. Kaviani, and P. E. Barclay, Single-crystal diamond nanobeam waveguide optomechanics, Phys. Rev. X **5**, 041051 (2015).

[56] K. Bai, Z. Peng, H.-G. Luo, and J.-H. An, Retrieving ideal precision in noisy quantum optical metrology, Phys. Rev. Lett. **123**, 040402 (2019).

[57] W.-L. Song, H.-B. Liu, B. Zhou, W.-L. Yang, and J.-H. An, Remote charging and degradation suppression for the quantum battery, Phys. Rev. Lett. **132**, 090401 (2024).

[58] J. Q. You and F. Nori, Quantum information processing with superconducting qubits in a microwave field, Phys. Rev. B **68**, 064509 (2003).

[59] I. Chiorescu, P. Bertet, K. Semba, Y. Nakamura, C. Harmans, and J. Mooij, Coherent dynamics of a flux qubit coupled to a harmonic oscillator, Nature (London) **431**, 159 (2004).

[60] A. Wallraff, D. I. Schuster, A. Blais, L. Frunzio, R.-S. Huang, J. Majer, S. Kumar, S. M. Girvin, and R. J. Schoelkopf, Strong coupling of a single photon to a superconducting qubit using circuit quantum electrodynamics, Nature (London) **431**, 162 (2004).

[61] M. Z. Weng, T. Tian, and Z. H. Wang, Vibration induced transparency: Simulating an optomechanical system via the cavity QED setup with a movable atom, Fundam. Res. **3**, 50 (2023).

[62] M. A. Sillanpää, J. I. Park, and R. W. Simmonds, Coherent quantum state storage and transfer between two phase qubits via a resonant cavity, Nature (London) **449**, 438 (2007).

[63] J. Q. You and F. Nori, Superconducting circuits and quantum information, Phys. Today **58**(11), 42 (2005).

[64] Z. Liu and G. Hanna, Population and energy transfer dynamics in an open excitonic quantum battery, Molecules **29**, 889 (2024).

[65] J. Q. Quach and W. J. Munro, Using dark states to charge and stabilize open quantum batteries, Phys. Rev. Appl. **14**, 024092 (2020).

[66] F.-Z. Ji, S.-Y. Bai, and J.-H. An, Strong coupling of quantum emitters and the exciton polariton in MoS_2 nanodisks, Phys. Rev. B **106**, 115427 (2022).

[67] H.-B. Liu, W. L. Yang, J.-H. An, and Z.-Y. Xu, Mechanism for quantum speedup in open quantum systems, Phys. Rev. A **93**, 020105(R) (2016).

[68] H.-P. Breuer and F. Petruccione, *The Theory of Open Quantum Systems* (Oxford University Press, Oxford, 2002).